

Raman scattering in hexagonal InN under high pressure

C. Pinquier, F. Demangeot, and J. Frandon

Laboratoire de Physique des Solides, UMR 5477, IRSAMC, Université Paul Sabatier, 118 route de Narbonne, 31062 Toulouse Cedex 4, France

J. W. Pomeroy and M. Kuball

H. H. Wills Physics Laboratory, University of Bristol, Bristol BS8 1TL, United Kingdom

H. Hubel, N. W. A. van Uden, and D. J. Dunstan

Physics Department, Queen Mary and Westfield College, University of London, London E1 4NS, United Kingdom

O. Briot, B. Maleyre, S. Ruffenach, and B. Gil

Groupe d'Etude des Semiconducteurs, Université Montpellier II, Case Courrier 074, 34095 Montpellier Cedex 5, France

(Received 19 March 2004; revised manuscript received 21 May 2004; published 17 September 2004)

The behavior of the E_2 and $A_1(\text{LO})$ optical phonons of hexagonal indium nitride under hydrostatic pressure was studied using Raman spectroscopy. Linear pressure coefficients and the corresponding Grüneisen parameters for both modes were determined for the wurtzite structure up to 11.6 GPa, close to the starting pressure of the hexagonal to rocksalt phase transition of InN. Raman spectra acquired within the 11.6 to 13.2 GPa pressure range suggest that wurtzite InN undergoes a gradual phase transition, and the reverse transformation exhibits a strong hysteresis effect during the downstroke.

DOI: 10.1103/PhysRevB.70.113202

PACS number(s): 63.20.-e, 61.50.Ks

I. INTRODUCTION

Due to their extensive use for optoelectronic devices, hexagonal III-V semiconductors have been intensively studied during the last several years. They are obtained as layers, grown on various buffer layers and substrates. Therefore they are usually strained, because of the significant lattice mismatch of materials involved in the heterostructures. The internal stress is currently assumed to be biaxial, and Raman spectroscopy can be employed for measuring the built-in strain in such samples. Data required for this evaluation are the deformation potentials of phonons, especially those of the nonpolar high frequency E_2 phonon, which is detected in the straightforward $z(xx)\bar{z}$ geometry, and exhibits a high scattering cross section even far away from resonant conditions. The deformation potentials have been already determined for wurtzite GaN^{1,2} and AlN^{3,4} by a combination of accurate Raman measurements performed under hydrostatic pressure and biaxial stress.

The growth of thick undoped InN layers characterized by high structural quality is still very difficult.⁵ Therefore, to date, the knowledge of physical properties of InN remains rather poor. For example, its fundamental electronic band gap energy is controversial.⁶ Concerning its lattice dynamical properties, the zone-center phonon frequencies have been measured for wurtzite^{7,8} and cubic⁹ InN. In order to determine the corresponding deformation potentials, it is first necessary to perform Raman experiments under hydrostatic pressure on bulk crystals. In fact, such data are not available because bulk InN material has not been fabricated so far. Darakchieva *et al.*¹⁰ published recently the deformation potentials of E_2 and $E_1(\text{TO})$ phonons. However, due to the lack of experimental data, they used the Grüneisen parameters and bulk moduli calculated by Kim *et al.*¹¹

In this paper, we report a study of the E_2 and $A_1(\text{LO})$ phonons of InN under hydrostatic pressure, up to 13.2 GPa. The measurements were performed in a pressure cell, on small InN flakes previously removed from a thick high quality InN layer grown by metalorganic vapor phase epitaxy (MOVPE). Hydrostatic pressure coefficients and mode Grüneisen parameters of InN phonons are determined. A gradual phase transition of InN is evidenced for pressures around 11.6 GPa.

II. EXPERIMENT

The sample used for this study is a 1- μm -thick wurtzite InN layer, grown on a sapphire substrate by MOVPE.¹² The electron density was determined by Hall measurements to be $2.3 \times 10^{19} \text{ cm}^{-3}$, which is typical for current InN material.¹³

Pressure was generated by a diamond anvil cell (DAC), warranting hydrostatic conditions up to ~ 13 GPa. The pressure transmitting medium was argon. The hydrostatic pressure, together with experimental uncertainties, were determined using the ruby luminescence method¹⁴ at the beginning and at the end of the acquisition time. Due to the different elastic properties of InN and sapphire, free-standing InN is required for the measurements, and it was fabricated by scraping a razor blade over the sample surface, resulting in InN flakes of about 10- μm -diam size. The micro-Raman spectra of the InN sample and the ruby luminescence were recorded using a Renishaw spectrometer equipped with holographic notch filters and a CCD camera, together with a Leica microscope with a $20\times$ long focal objective. A 632.8 nm He-Ne laser with 25 mW output power was used as excitation source. The spectra were recorded in back-scattering geometry, with a typical resolution of 1 cm^{-1} on

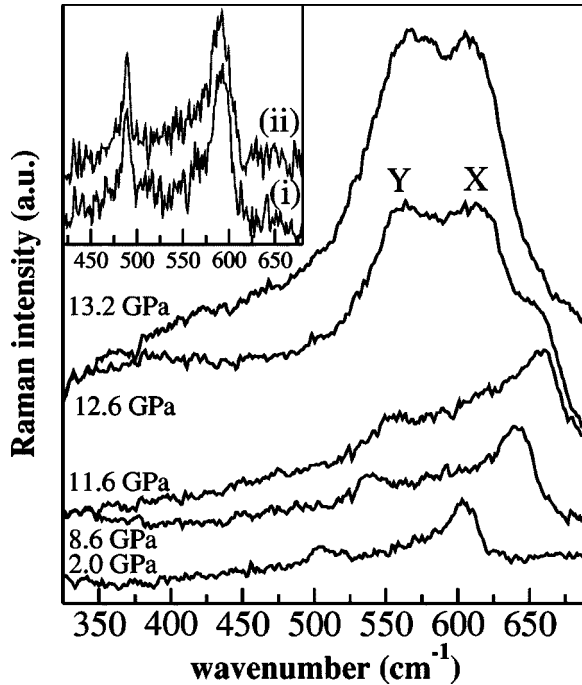


FIG. 1. Raman spectra recorded under hydrostatic pressure in backscattering geometry. Spectra in the insert were recorded before (i) and after (ii) the pressure experimental run.

measured frequencies due to the instrument. The acquisition time for all spectra was 20 min. Finally, the diamond luminescence background was subtracted from the recorded Raman spectra.

The Raman spectrum (i) shown in the insert of Fig. 1 was acquired on a single free-standing InN flake under atmospheric pressure, outside the DAC. The two main peaks, observed at 490 and 591 cm^{-1} , are assigned to the long-wavelength E_2 and $A_1(\text{LO})$ (longitudinal optical) phonons of InN, respectively, in agreement with Raman selection rules for the wurtzite structure. The measured frequencies are lower than those of the InN layer on the sapphire substrate [491 and 592 cm^{-1} , respectively], due to the relaxation of the compressive strain. The residual deformation of the flakes is very weak, as can be deduced from the measured phonon frequencies. Actually, the spectral width of the E_2 phonon (7 cm^{-1}) in the current Raman spectrum is larger than that measured with the best InN layers investigated up to now⁶ (4 cm^{-1}), attesting that the structural quality of the present sample is slightly lower. This is likely due to the large thickness of the epilayer under study. The intensity of the $A_1(\text{LO})$ mode is particularly important, which has been already observed in several InN layers.¹⁵ Actually, due to its location in the spectrum, the latter feature is assigned to a coupled plasmon-phonon mode arising from nonconserving wave-vector scattering processes, as suggested by Kasic *et al.*¹⁶ Finally, in spectra recorded outside the DAC, a shoulder is hardly observed at 565 cm^{-1} on the low frequency side of the LO phonon. It is tentatively assigned to the silent B_1 phonon of the wurtzite structure, likely disorder activated, in view of the good agreement between the frequency at zero pressure and calculated data.⁸

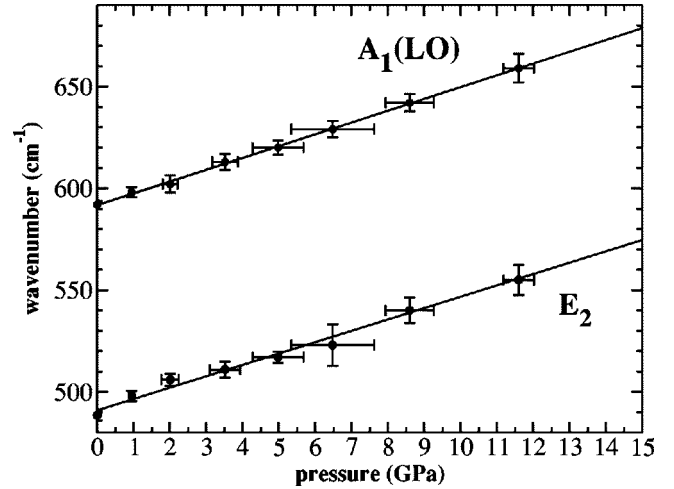


FIG. 2. InN wurtzite phonon wave numbers versus hydrostatic pressure in the upstroke.

III. RESULTS AND DISCUSSION

Figure 1 displays Raman spectra recorded with increasing pressure up to 13.2 GPa, at which point the gasket was severely deformed. Therefore, it is the highest pressure that was reached in the DAC. An increase in phonon frequencies with applied pressure is observed. At pressures higher than 12 GPa, the $A_1(\text{LO})$ mode is vanishing and a new mode labeled X of strong intensity is observed at 610 cm^{-1} . At the same time, another new mode Y shows up at 570 cm^{-1} with a similar intensity. We note that phonon lines are found significantly broader inside the DAC than under ambient conditions: this is mainly due to the pressure variation during the acquisition of the spectrum. We concentrate first on the pressure range up to 11.6 GPa, while changes in the Raman spectrum at higher pressures related to the phase transformation of InN will be discussed later.

Experimental spectra were fitted by two Lorentzian-Gaussian peaks, in order to extract the frequencies of the observed modes. The frequency variation of these modes versus hydrostatic pressure is shown in Fig. 2, together with experimental uncertainties. Error bars in abscissas correspond to variations of pressure during the acquisition time of spectra. For most semiconductors, pressure dependence of phonon frequencies is usually modeled by a quadratic relationship. However, the second order term was found negligible in the present case. Therefore, we only give linear terms:

$$\omega = \omega_0 + K^H p,$$

where ω_0 is the phonon frequency at zero pressure, p is the hydrostatic pressure, and $K^H = (\partial\omega/\partial p)_{p=0}$ is the hydrostatic linear pressure coefficient.

Regression results are presented in Table I. The zero pressure phonon frequencies agree well with previous data reported in the literature.⁸

For the E_2 phonon, the present value of K^H (5.6 $\text{cm}^{-1} \text{GPa}^{-1}$) can be compared to that derived from its deformation potentials obtained by Darakchieva *et al.*¹⁰

TABLE I. Results of the linear regression (ω_0 and K^H) and calculated mode Grüneisen parameters γ .

Phonon mode	ω_0 (cm^{-1})	K^H ($\text{cm}^{-1} \text{GPa}^{-1}$)	γ
E_2	491.0	5.6	1.66
$A_1(\text{LO})$	591.7	5.8	1.43

($5.0 \text{ cm}^{-1} \text{GPa}^{-1}$). Mode Grüneisen parameters were determined from the pressure coefficients using the relation:

$$\gamma = - \frac{\partial \ln \omega}{\partial \ln V} = \frac{B_0}{\omega_0} K^H,$$

where the bulk modulus B_0 is the inverse of the isothermal compressibility. Experimental measurements on B_0 by x-ray diffraction have been reported by Ueno *et al.*¹⁷ ($B_0 = 125.5 \text{ GPa}$), and theoretical values by Perlin *et al.*¹⁸ ($B_0 = 165 \text{ GPa}$). The bulk modulus can also be evaluated from the elastic constants calculated by Kim *et al.*,¹¹ finding a value of $B_0 = 146 \text{ GPa}$, in excellent agreement with previous theoretical work¹⁹ ($B_0 = 144 \text{ GPa}$). Mode Grüneisen parameters determined using $B_0 = 146 \text{ GPa}$ are given in Table I. The bulk modulus is smaller in the case of InN, compared to GaN and AlN,¹⁹ attesting to its higher compressibility, and InN mode Grüneisen parameters are higher than for GaN and AlN.^{20,21}

A close inspection of the experimental results reveals that a change occurred for pressures above 11.6 GPa, with the appearance of the two features previously mentioned. The frequency of the structure labeled Y is close to that of the E_2 phonon of InN under pressure. In addition, no significant shift of the X mode is evidenced for $p = 11.6 \text{ GPa}$. The disappearing of the LO mode at 13.2 GPa cannot be correlated to any change in the carrier density. From theoretical and experimental studies, the pressure of the wurtzite to rocksalt structure phase transition of InN is estimated in the 10–15.5 GPa range.^{17,19,23–25} However, first order Raman scattering is forbidden by selection rules in the case of the rocksalt structure,²⁶ whereas a signal of increasing intensity is still recorded at high pressure. This suggests that the phase transformation hardly begins at about 11.6 GPa. The material undergoes a gradual intermediate transformation which corresponds to the isostructural transition of the wurtzite cell previously proposed by Bellaïche *et al.*²³ from first-principle calculations: gliding of In and N sublattices under hydrostatic pressure induces a continuous variation of the angle between In-N bounds, before the rocksalt structure is completed. Another signature of such a gradual transformation in

the same pressure range has been found by Ueno *et al.*,¹⁷ who have reported a clear change in the variation of the c/a ratio of the wurtzite structure under hydrostatic pressure.

Another explanation of the experimental results can be proposed: if the rocksalt structure is almost completed at 13.2 GPa, structural disorder of this material may give rise to broad Raman lines, roughly reproducing the phonon density of states of the rocksalt phase. However, this assumption does not seem in agreement with the final recovery of the initial Raman spectrum: indeed, the one obtained under ambient conditions, after the cycle of pressure variation, was identical to that recorded before introducing the sample into the DAC, see spectrum (ii) in the insert of Fig. 1. In any case, the strong signal recorded at high pressure may be tentatively assigned to an increase of the volume probed by the incident light beam, due to a significant decrease of the absorption coefficient of InN.

After reaching 13.2 GPa, four spectra were recorded in the downstroke, with the lowest pressure before opening the DAC of 3 GPa. A clear hysteresis effect was observed: the $A_1(\text{LO})$ mode was not evidenced, even at 3 GPa, with a decreasing intensity of the whole spectrum, which suggests that the reverse transition is not completed. These observations are in agreement with experimental results deduced from energy dispersive x-ray diffraction.²⁴ In fact, a similar hysteresis effect has been reported by Perlin *et al.*²² for bulk GaN: the reverse rocksalt to wurtzite transition beginning at 30 GPa was over at 20 GPa only. However, in this case the downstroke evolution was associated with an irreversible transformation of the original GaN single crystal into a nanocrystalline sample. In contrast, as mentioned previously, the transformation of the InN under hydrostatic pressure is found reversible, without any amorphization effects. The observed hysteresis can be associated with the gradual transformation evidenced at the upstroke already discussed. Further studies are now in progress, in order to investigate these effects.

IV. CONCLUSION

In summary, we investigated the influence of hydrostatic pressure (up to 13.2 GPa) on optical phonons of wurtzite InN by means of Raman scattering. These experiments allowed one to derive the Grüneisen parameters for the E_2 and $A_1(\text{LO})$ modes, which are, respectively, 1.66 and 1.43 using the value of 146 GPa for the bulk modulus. A phase transition in the high pressure range is clearly observed. In the future, the deformation potentials of the E_2 and $A_1(\text{LO})$ phonons could be evaluated by combining the present results with Raman and x-ray studies of biaxially strained InN layers.

¹F. Demangeot, J. Frandon, P. Baules, F. Natali, F. Semond, and J. Massies, *Phys. Rev. B* **69**, 155215 (2004).

²V. Y. Davydov, N. S. Averkiev, I. N. Goncharuk, D. K. Nelson, I. P. Nikitina, A. S. Polovnikov, A. N. Smirnov, and M. A. Jacob-

son, *J. Appl. Phys.* **82**, 5097 (1997).

³J. Gleize, M. A. Renucci, J. Frandon, E. Bellet-Amalric, and B. Daudin, *J. Appl. Phys.* **93**, 2065 (2003).

⁴A. Sarua, M. Kuball, and J. E. Nostrand, *Appl. Phys. Lett.* **81**,

- 1426 (2002).
- ⁵Y. Nanishi, Y. Saito, and T. Yamaguchi, *J. Appl. Phys.* **42**, 2549 (2003).
- ⁶O. Briot, B. Maleyre, S. Clur-Ruffenach, B. Gil, C. Piquier, F. Demangeot, and J. Frandon, *Phys. Status Solidi C* **1**, 1425 (2004).
- ⁷V. Y. Davydov, V. V. Emtsev, I. N. Goncharuk, A. N. Smirnov, V. D. Petrikov, V. V. Mamutin, V. A. Vekshin, and S. N. Ivanov, *Appl. Phys. Lett.* **75**, 3297 (1999).
- ⁸G. Kaczmarczyk, A. Kaschner, S. Reich, A. Hoffmann, C. Thomsen, D. J. As, A. P. Lima, D. Schikora, K. Lischka, R. Averbeck, and H. Riechert, *Appl. Phys. Lett.* **76**, 2122 (2000).
- ⁹A. Tabata, A. P. Lima, L. K. Teles, L. M. R. Scolfaro, J. R. Leite, V. Lemos, B. Schöttker, T. Frey, D. Schikora, and K. Lischka, *Appl. Phys. Lett.* **74**, 362 (1999).
- ¹⁰V. Darakchieva, P. P. Paskov, E. Valcheva, T. Paskova, B. Monemar, M. Schubert, H. Lu, and W. Shaff, *Appl. Phys. Lett.* **84**, 3636 (2004).
- ¹¹K. Kim, W. R. L. Lambrecht, and B. Segall, *Phys. Rev. B* **53**, 16310 (1996).
- ¹²B. Maleyre, O. Briot, and S. Ruffenach, *J. Cryst. Growth* (to be published).
- ¹³A. G. Bhuiyan, A. Hashienoto, and A. Yamamoto, *J. Appl. Phys.* **94**, 2779 (2003).
- ¹⁴H. K. Mao, P. M. Bell, J. W. Shaner, and D. J. Steinberg, *J. Appl. Phys.* **49**, 3276 (1978).
- ¹⁵M. Kuball, J. W. Pomeroy, M. Wintrebart-Fouquet, K. S. A. Butcher, H. Lu, and W. J. Schaff, *J. Cryst. Growth* (submitted).
- ¹⁶A. Kasic, M. Schubert, Y. Saito, Y. Nanishi, and G. Wagner, *Phys. Rev. B* **65**, 115206 (2002).
- ¹⁷M. Ueno, M. Yoshida, A. Onodera, O. Shimomura, and K. Takemura, *Phys. Rev. B* **49**, 14 (1994).
- ¹⁸P. Perlin, I. Gorczyca, I. Gregory, T. Suski, N. E. Christensen, and A. Polian, *Jpn. J. Appl. Phys., Suppl.* **32**(1), 334 (1993).
- ¹⁹J. Serrano, A. Rubio, E. Hernandez, A. Munoz, and A. Mujica, *Phys. Rev. B* **62**, 16612 (2000).
- ²⁰A. R. Goñi, H. Siegle, K. Syassen, C. Thomsen, and J. M. Wagner, *Phys. Rev. B* **64**, 035205 (2001).
- ²¹M. Kuball, J. M. Hayes, A. D. Prins, N. W. A. van Uden, D. J. Dunstan, Y. Shi, and J. H. Edgar, *Appl. Phys. Lett.* **78**, 724 (2001).
- ²²P. Perlin, C. Jaubertie-Carillon, J. P. Itie, A. San Miguel, I. Grzegory, and A. Polian, *Phys. Rev. B* **45**, 83 (1992).
- ²³L. Bellaiche, K. Kunc, and J. M. Besson, *Phys. Rev. B* **54**, 8945 (1996).
- ²⁴Q. Xia, H. Xia, and A. L. Ruoff, *Mod. Phys. Lett. B* **8**, 345 (1994).
- ²⁵S. Uehara, T. Masamoto, A. Onodera, M. Ueno, O. Shimomura, and K. Takemura, *J. Phys. Chem. Solids* **58**, 2093 (1997).
- ²⁶P. T. C. Freire, M. A. Araújo Silva, V. C. S. Reynoso, A. R. Vaz, and V. Lemos, *Phys. Rev. B* **55**, 6743 (1997).